

Supporting Information

Electrical-Pumping Spasing Action from Cross-Stacked Microwires

Zhanguo Li,^{a,b} Gaohang He,^c Mingming Jiang,^{*,a,d} Jiaolong Ji,^d Chongxin Shan,^{*,a,e} and Dezhen Shen^{*,a}

^a State Key Laboratory of Luminescence and Applications, Changchun Institute of Optics, Fine Mechanics and Physics, Chinese Academy of Sciences, No.3888 Dongnanhu Road, Changchun, 130033, China

^b University of Chinese Academy of Sciences, Beijing 100049, China.

^c Vacuum Interconnected Nanotech Workstation, Suzhou Institute of Nano-Tech and Nano-Bionics, Chinese Academy of Sciences, Suzhou 215123, China

^d College of Science, Nanjing University of Aeronautics and Astronautics, No. 29 Jiangjun Road, Nanjing 210016, China

^e School of Physics and Engineering, Zhengzhou University, Zhengzhou 450001, China

*Email: mmjiang@nuaa.edu.cn; cxshan@zzu.edu.cn; shendz@ciomp.ac.cn

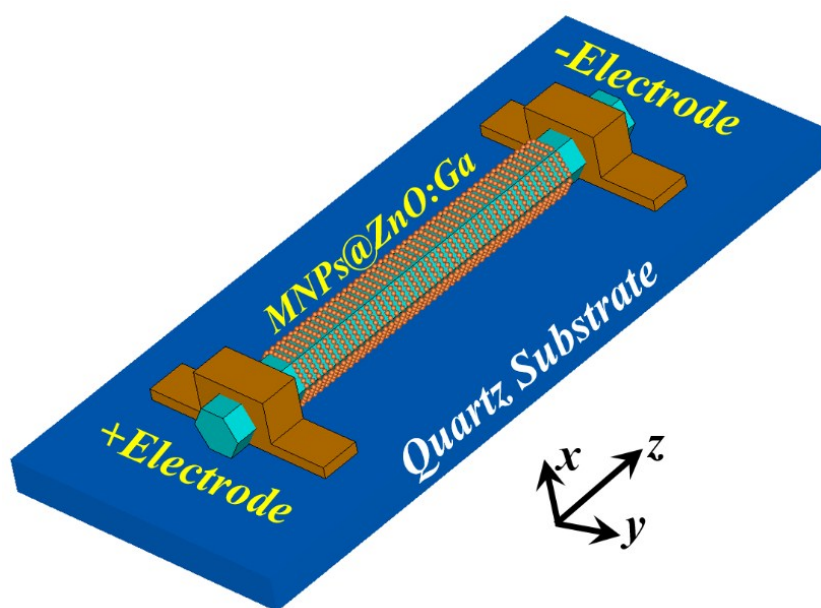


Figure S1. Schematic diagram of typical incandescent light source, which composed of single Ga-doped ZnO microwire (ZnO:Ga MW) prepared with metal nanostructures decoration.

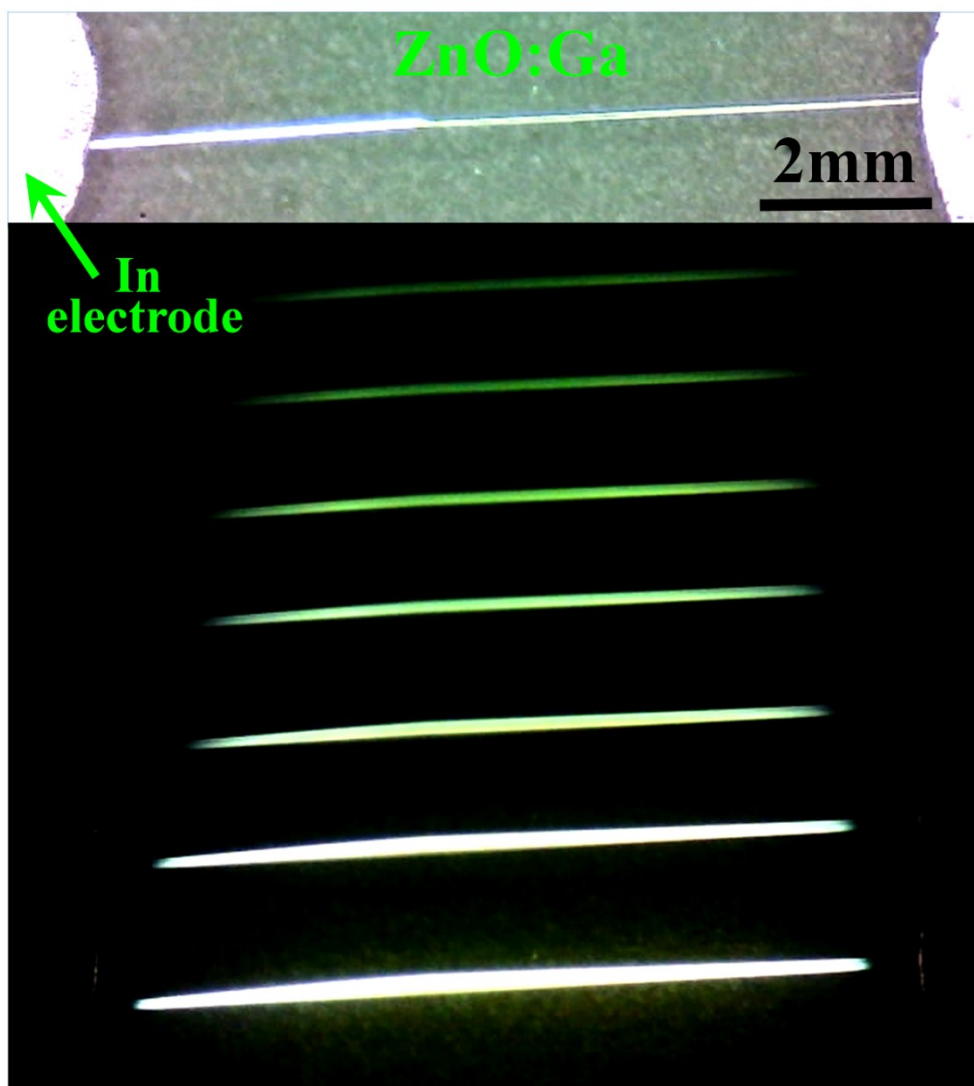


Figure S2. Single ZnO:Ga MW (weight ratios of ZnO:Ga₂O₃:C=10:1:11) was successfully synthesized, and then selected to construct an incandescent-type light source. When the injection current reached a certain value, the ZnO:Ga MW begins to emit green light, with the emission region located towards the center. Increasing the injection current can lead to enhancement of the brightness and emission regions, accompanied by the injection current ranging from 1.25 mA to 2.5 mA.

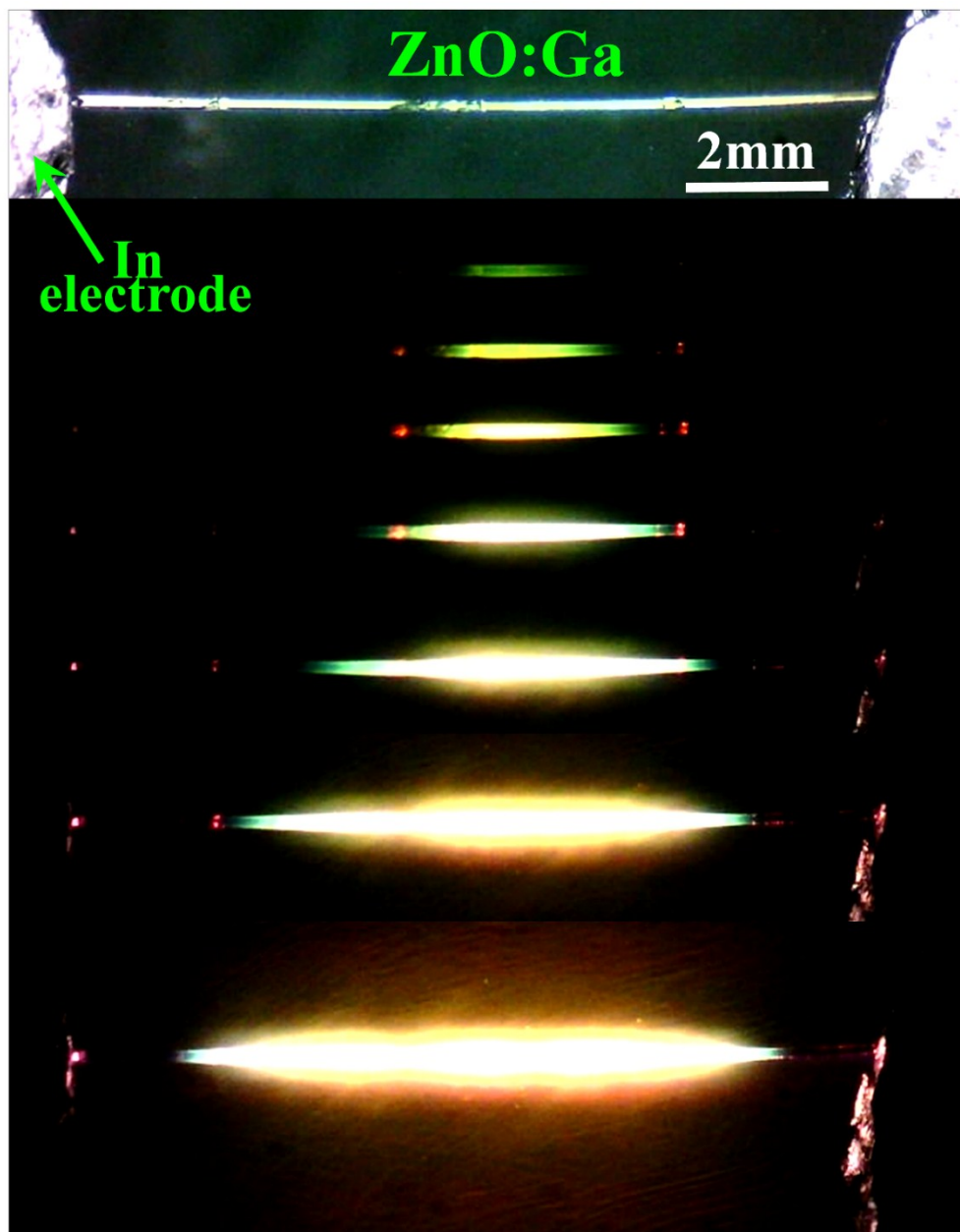


Figure S3. Single ZnO:Ga MW (The weight ratios of ZnO:Ga₂O₃:C=9:1:10) was selected to construct an incandescent-type light source. The single ZnO:Ga MW begins to emit green light when the injection current reached a certain value, with corresponding emission regions located towards the center. Increasing the injection current can lead to enhancement of the brightness and emission regions. Meanwhile, the brightest spot of the emission is always located towards the center. The injection currents ranged from 2.15 mA to 3.5 mA.

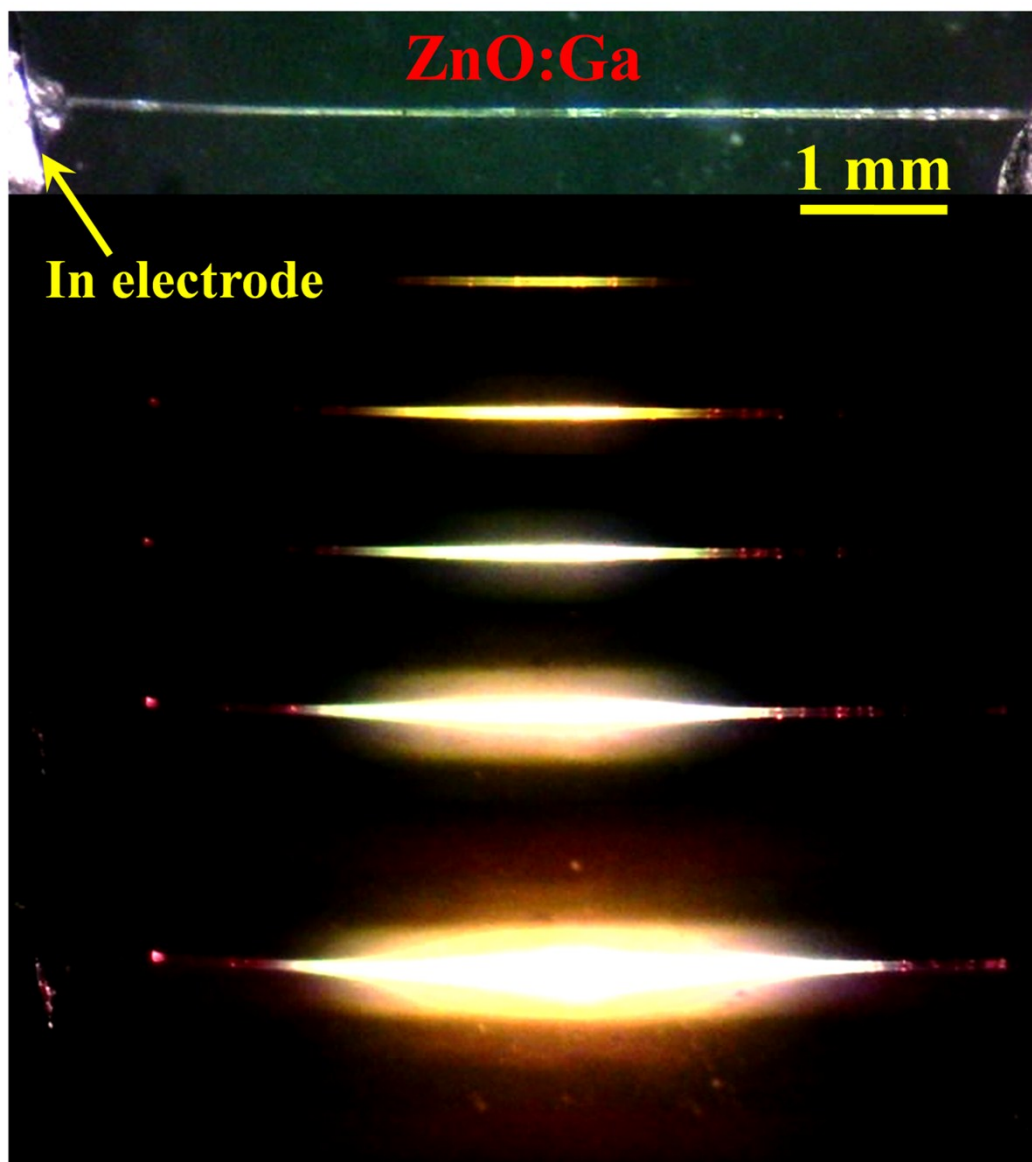


Figure S4. Single ZnO:Ga MW (The weight ratios of ZnO:Ga₂O₃:C=8:1:9) was selected to construct an incandescent-type light source. The single ZnO:Ga MW begins to emit visible light when the injection current exceeded a certain value, with the emission regions located towards the center. Increasing the injection current can lead to the enhancement of the brightness and emission regions. The brightest spot of the emission is always located towards the center. The injection currents ranged from 2.35 mA to 4.25 mA.

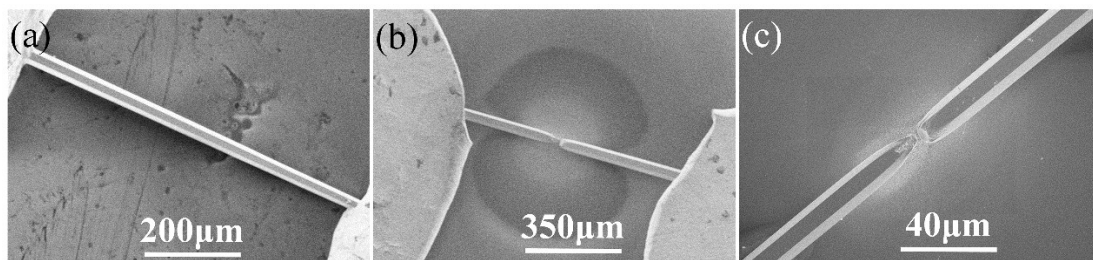


Figure S5. (a) SEM image of single ZnO:Ga MW based incandescent-type light source. (b) When the applied bias reached a certain value, electrical breakdown behavior can happen, with the broken region located towards the center. (c) Amplified SEM image of the broken region.

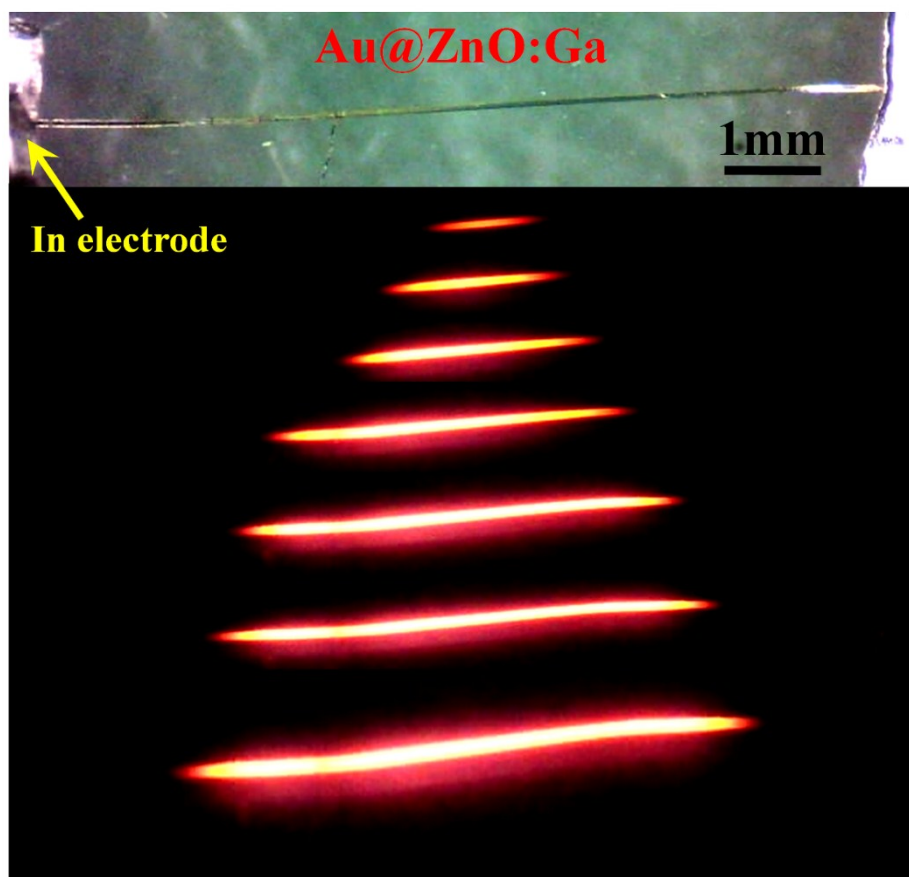


Figure S6. Single ZnO:Ga MW (The weight ratios of ZnO:Ga₂O₃:C=9:1:10) was selected to construct an incandescent-type light source. Introducing Au quasiparticle films decoration (Sputtering time: 60 s), hybrid architecture was fabricated (Au@ZnO:Ga). By applying bias onto the MW, single Au@ZnO:Ga MW begins to emit red lighting, the emission regions located towards the center of the wire. Increasing the injection current can lead to enhancement of the brightness and emission regions. The brightest spot of the emission is always located towards the center. The injection currents ranged from 5.0 mA to 6.5 mA.

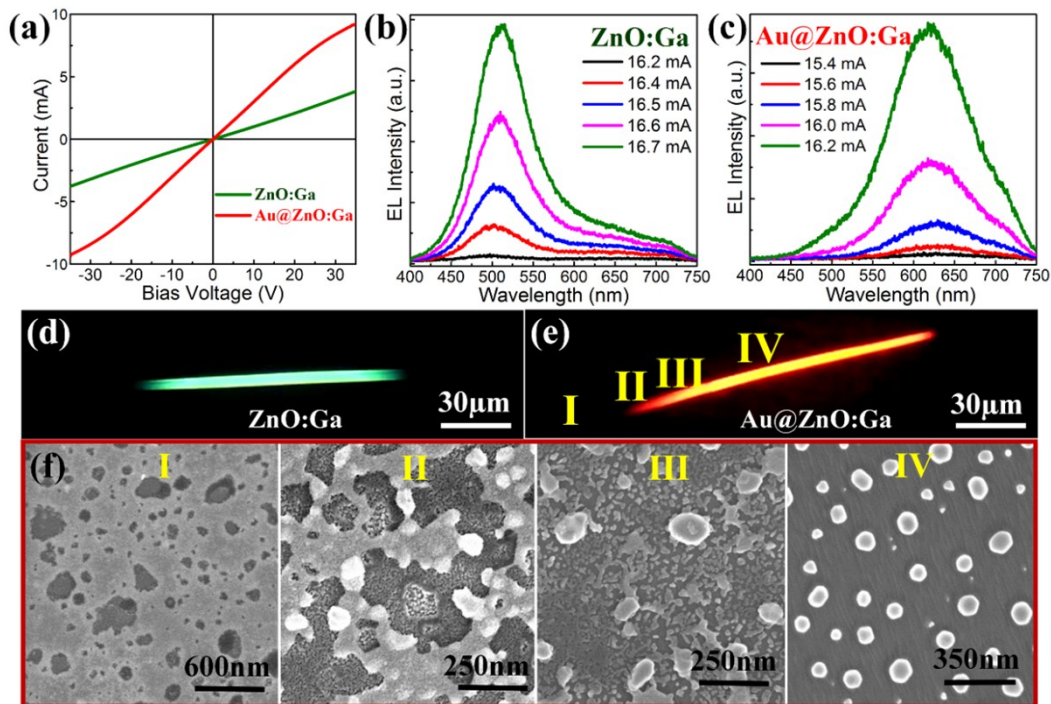


Figure S7. EL emission characteristics from single Au@ZnO:Ga MW based incandescent-type light source: (a) *I-V* characteristic of single ZnO:Ga MW prepared without, and with Au quasiparticle nanofilms decoration. (b) EL emissions from the single ZnO:Ga MW based incandescent-type light source, the dominating emission wavelengths centered at 510 nm. (c) EL emissions from single Au@ZnO:Ga MW based incandescent-type light source, the dominating emission wavelengths centered at 620 nm. (d) The typical optical microscopic images of EL emissions from single ZnO:Ga MW, with the emission regions located towards the center of the wire. (e) The typical optical microscopic image of EL emissions from Au@ZnO:Ga MW, with the emission regions located towards the center of the wire. In addition, regions denoted as **I**, **II**, **III** and **IV** were selected in accordance with the In-ZnO:Ga contact region, critical region between light-emitting or not, and light-emitting regions, respectively. (f) SEM images demonstrated the surface morphologies of Au nanostructures (Sputtering time: 60 s). The surface morphologies gradually varied from quasiparticle films (**I**), to the clusters consisting of quasiparticle films and isolated Au nanoparticles (**II**) and (**III**), and finally converted into physically isolated Au nanoparticles ($D \sim 100$ nm) aggregations (**IV**). *Therefore, hybrid architecture composed of physically isolated Au nanoparticles decorated ZnO:Ga MW (AuNPs@ZnO:Ga) can be fabricated.*

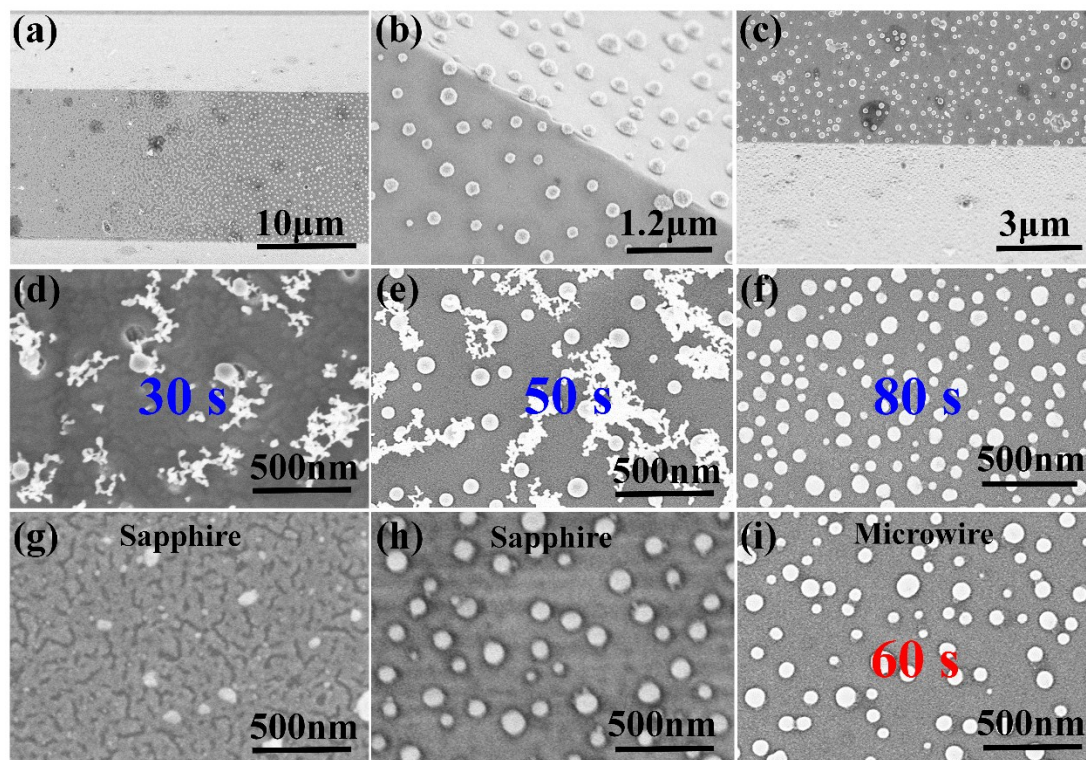


Figure S8. (a) The transition of Au nanostructures transferred from quasiparticle nanofilm into physically isolated nanoparticles, with the location towards the critical region between lighting or not (Sputtering time: 60 s). (b) SEM image of isolated Au nanoparticles located in the lighting regions (Sputtering time: 60 s). (c) Amplified SEM image of isolated Au nanoparticles, which located in the lighting regions (Sputtering time: 60 s). (d) Amplified SEM image of isolated Au nanoparticles located in the lighting regions (Sputtering time: 30 s). (e) Amplified SEM image of isolated Au nanoparticles located in the lighting regions (Sputtering time: 50 s). (f) Amplified SEM image of isolated Au nanoparticles located in the lighting regions (Sputtering time: 80 s). (g) SEM image of Au quasiparticle films, which evaporated on the sapphire substrate (Sputtering time: 60 s). (h) After annealing treatment (450 °C), Au quasiparticle films can be transferred into physically isolated Au nanoparticles ($D \sim 100$ nm). (i) Surface morphologies of isolated Au nanoparticles ($D \sim 100$ nm), which located in the lighting regions (Sputtering time: 60 s).

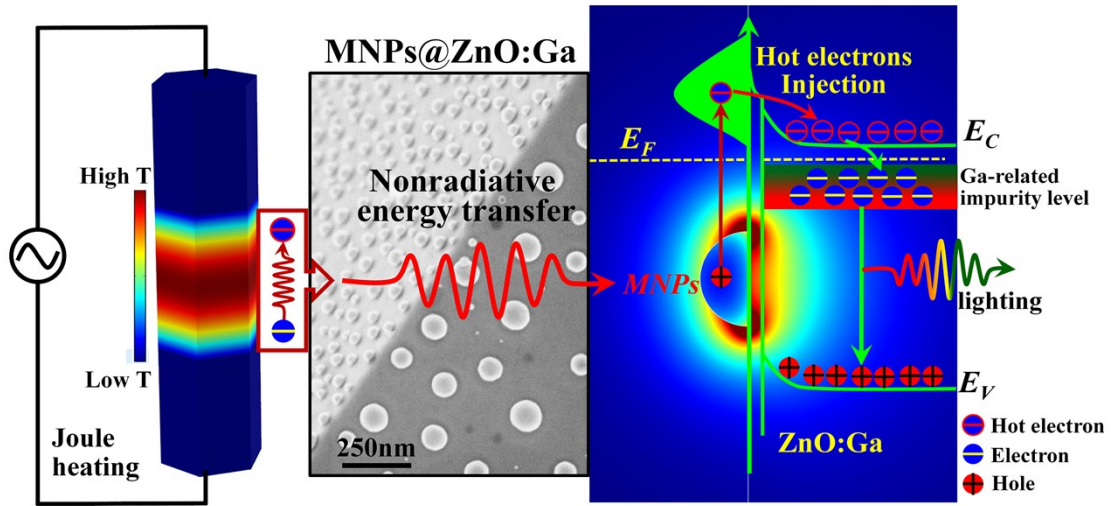


Figure S9. The light-emitting mechanism for Au-plasmon mediated EL emission characteristics from single AuNPs@ZnO:Ga MW based incandescent-type light source: (1) Due to Joule heating effect, the hottest spot formed towards the center of the MWs could provide a modest electrical field, thus the transported electrons can be accelerated and become energetic electrons; meanwhile, the Au quasiparticle film towards the hottest regions could be annealed into random isolated Au nanoparticles. (2) Au plasmons could be excited by means of impact ionization with energetic electrons transported in the MW-channel, and become spatially localized towards the center of the MWs. Thus, due to plasmonic decaying nonradiatively, a distribution of "hot electrons" well above the Schottky barrier at the Au-ZnO:Ga interface can be generated, and then can be directly injected into the conduction band of ZnO:Ga. (3) Subsequently, electrons are relaxed to Ga-related impurity levels, leading to modification of the impurity levels; in turn, radiative recombination can be modulated.

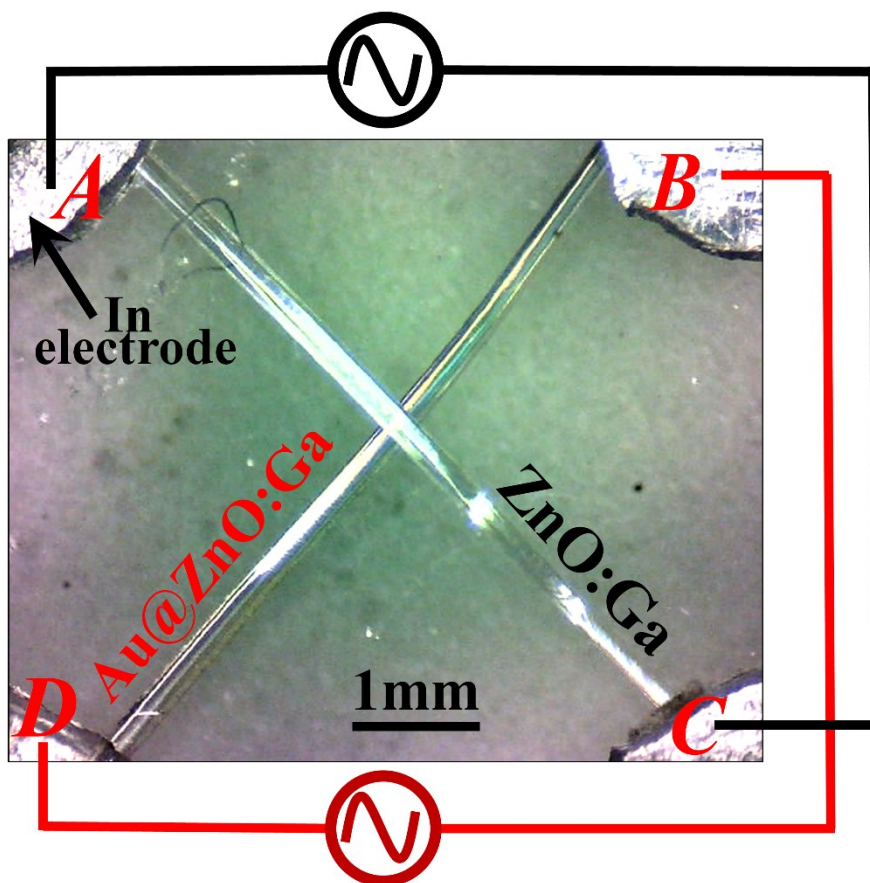


Figure S10. Optical microscope image of the cross-stacked architectures composed of single ZnO:Ga MW, crossed with the other AuNPs@ZnO:Ga MW. By applying bias onto both MWs respectively, EL emissions were observed from the cross-stacked architectures, with the emission regions located towards the crossed regions, respectively.

In this section, let's focus the attention on the crossed MWs based architecture, with light-emitting regions being separated from each other. Figure S10(a) demonstrated optical imaging of the crossed MWs based light-emitting device composed of a single bare ZnO:Ga MW, crossed with another ZnO:Ga MW via Au quasiparticle film decoration (Sputtering time: 60 s). When applied bias onto the bare MW, optical microscope image of bright and green lighting were captured. When applied bias onto both ends of the single AuNPs@ZnO:Ga MW, red lighting can be observed. In particular, when applied bias onto both ends of the crossed MWs simultaneously, for

example, **A-C**, and **B-D** respectively. Maintain the injection current of **A-C** a constant value ~ 4.5 mA, while increasing the injection current of **B-D** gradually, green and red lighting can be observed from the crossed MWs simultaneously. The lighting behaviors are completely independent from each other, as shown in Figures S11(d)-(i).

In addition, Figure S12(c) demonstrates I - V characteristics of a single bare ZnO:Ga MW (green solid line), single AuNPs@ZnO:Ga MW (red solid line), and the crossed MWs (blue solid line). It can be found out that I - V curves presented linear shape, indicating the formation of the Ohmic contacts between the In electrodes and MWs. Thus, there is almost impervious contributions to the I - V measurements based on the crossed-MWs architectures when both the emission regions separated from each other. Further to demonstrate the EL emission characteristics, Figure S12(d) demonstrates EL spectra from the single ZnO:Ga MW based incandescent-type emitter, with the dominated emission wavelengths centered at 505 nm. Figure S12(e) demonstrates EL spectra from the other single AuNPs@ZnO:Ga MW based incandescent-type emitter, with the dominated emission wavelengths firstly centered at 600 nm, and then blue shifted to be 523 nm with increasing injection currents. When we maintained the injection current a fixed value of the single AuNPs@ZnO:Ga MW, such as 12.5 mA, while increasing the injected current of the single ZnO:Ga MW ranging from 2.5 mA to 4.5 mA, Figure S12(f) demonstrated that the dominant emission wavelengths changed from 600 nm, and then finally centered at 510 nm. To increase the injection current of AuNPs@ZnO:Ga MW being 12.9 mA, the dominant emission wavelengths transferred from 600 nm, and then finally centered at 515 nm (Figure S12(g)).

Increasing the injection current of single AuNPs@ZnO:Ga MW to be 13.1 mA, the dominating emission peaks of the crossed architecture centered at 518 nm (Figure S12(h)); Finally, when the injected current of single AuNPs@ZnO:Ga MW increased to be 13.3 mA, the emission peaks of the crossed MWs based light-emitting device centered at 520 nm (Figure S12(i)). Although, both the crossed MWs retained their independence on the EL emission characteristics, the integrated EL emission characteristics of the crossed MWs devices still could be tuned.

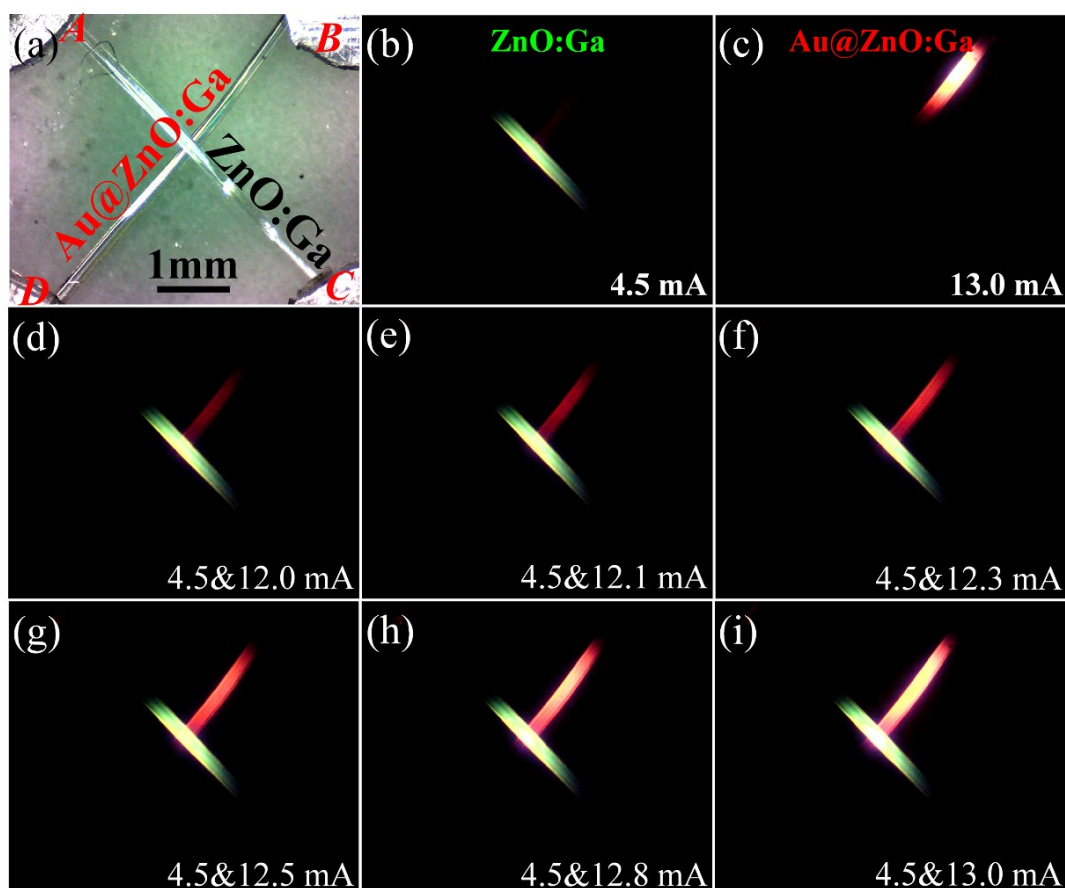


Figure S11. EL emissions from the cross-stacked architectures composed of single ZnO:Ga MW, crossed with the other AuNPs@ZnO:Ga MW, with the emission regions separated from each other: (a) The typical optical microscope image of the cross-stacked architecture. (b) When applied bias onto the single bare ZnO:Ga MW, EL emissions can be observed, the green brightness and emission regions increasing with the drain currents. (c) When applied bias onto AuNPs@ZnO:Ga MW, EL emissions can be observed, the red brightness and emission regions

increasing with the drain currents. When maintained the injection current of the ZnO:Ga MW a fixed value, such as 4.5 mA, while increasing the injection current of single AuNPs@ZnO:Ga MW ranging from 12.0 mA (d) to 13.0 mA (i). The cross-stacked architecture begins to emit visible light once the injection current exceeds a threshold value, accompanied with its increasing of the red brightness and emission regions.

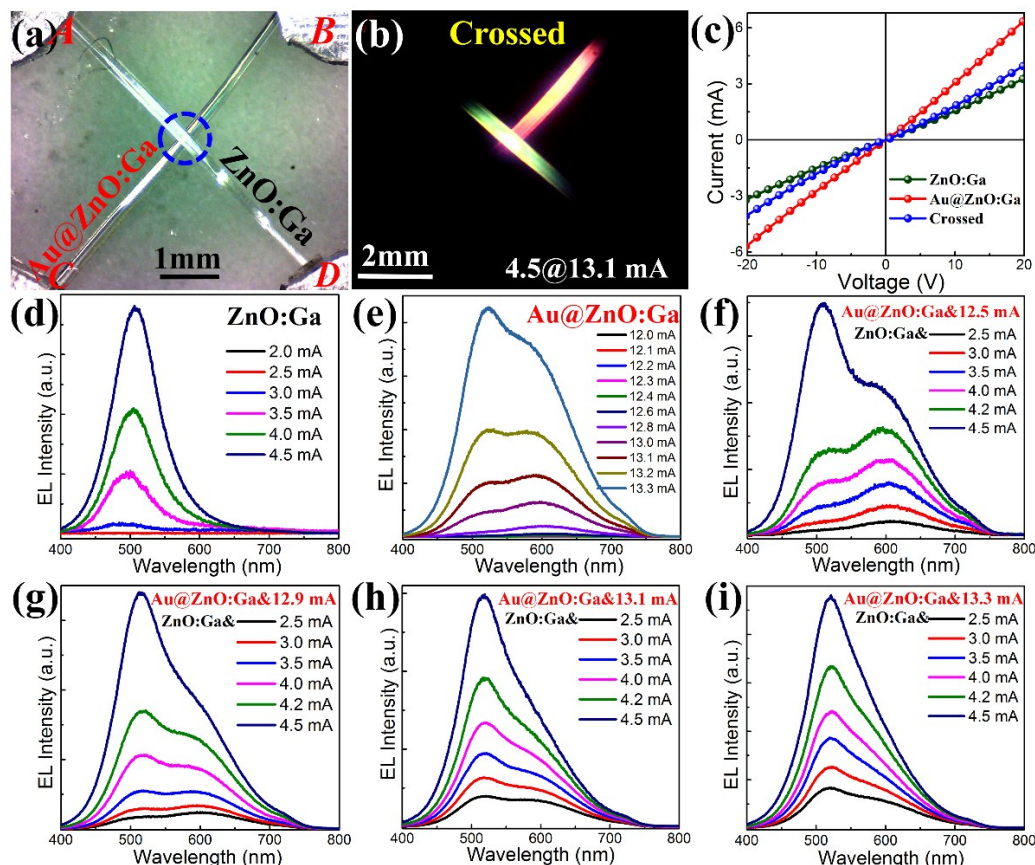


Figure S12. EL emissions from the cross-stacked architecture composed of single ZnO:Ga MW, crossed with the other AuNPs@ZnO:Ga MW, with the emission regions separated from each other: (a) The typical optical microscope image of the cross-stacked architecture. (b) The typical optical microscope images of light-emitting from the cross-stacked architecture when applied bias onto both ends of the crossed MWs. (c) I-V characteristics of the bare ZnO:Ga MW, AuNPs@ZnO:Ga MW, and the cross-stacked architecture, respectively. (d) EL emissions from single ZnO:Ga MW based incandescent-type emitter, the dominant emission wavelengths centered at 505 nm. (e) EL emissions from single AuNPs@ZnO:Ga MW based incandescent-type emitter, the dominant emission wavelengths firstly centered at 600 nm, and then centered at 523 nm with continue to increase the injection current. The emitted photons were also collected from electrically driven the cross-stacked architecture when applied bias onto both end of the crossed

MWs simultaneously. With increasing the injection current of the single ZnO:Ga MW ranging from 2.5 mA to 4.5 mA, while maintained the injection current of the other AuNPs@ZnO:Ga MW a fixed value, such as (f) 12.5 mA, the dominant emission wavelengths were firstly centered at 600 nm, and then turned to 510 nm; (g) 12.9 mA, the dominated emission wavelengths were firstly centered at 600 nm, and then blueshifted to be 515 nm; (h) 13.1 mA, the dominated emission wavelengths were firstly centered at 600 nm, and finally blueshifted to be 518 nm; (i) 13.3 mA, the dominated emission wavelengths firstly centered at 600 nm, and finally blueshifted to be 520 nm.

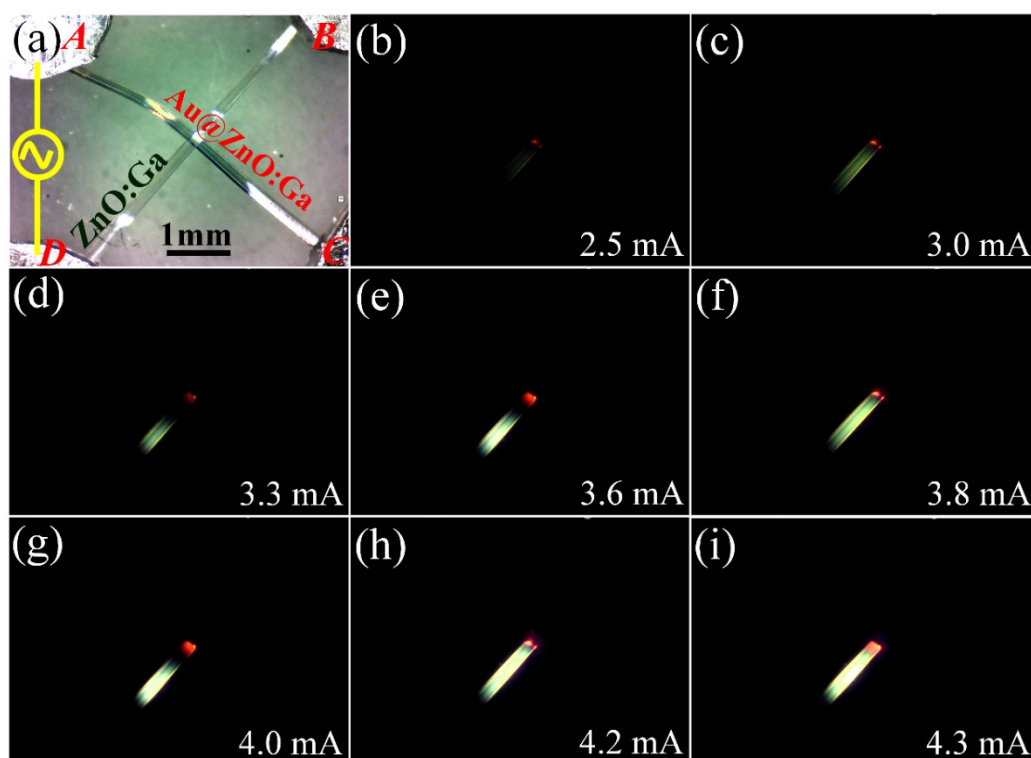


Figure S13. EL emissions from the cross-stacked architecture composed of single ZnO:Ga MW crossed with the other AuNPs@ZnO:Ga MW, when applied bias onto the electrodes *A* and *D*: (a) The typical optical microscope image of the cross-stacked architecture. When applied voltages onto the In electrodes *A* and *D*, the crossed architectures begins to emit green lighting, which located toward the section of the bare ZnO:Ga MW when the injected current exceeds a certain value. The brightness and light-emitting regions increased with the drain currents ranged from 2.5 mA to 4.3 mA. The brightest spots of the emission is always located the section of the bare MW.

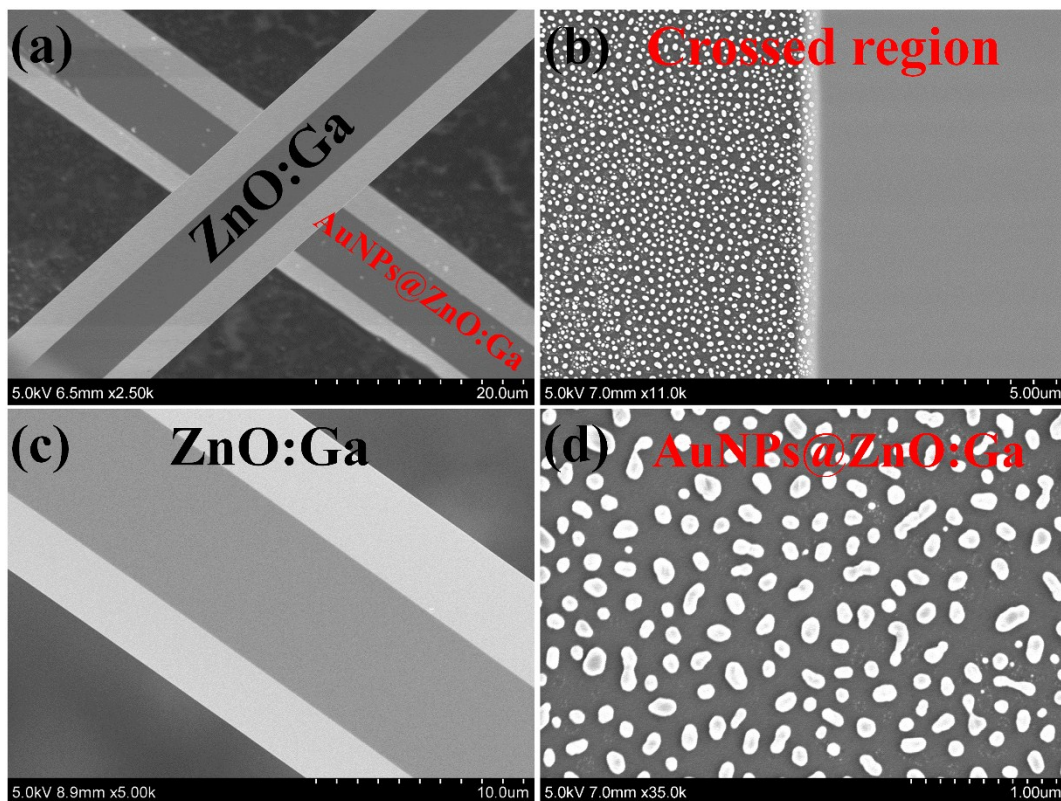


Figure S14. (a) SEM image of the cross-stacked architecture composed of single ZnO:Ga MW crossed with the other AuNPs@ZnO:Ga MW. (b) SEM image of the crossed regions of the cross-stacked architecture. (c) SEM image of bare ZnO:Ga MW, displayed smooth surfaces. (d) Physically isolated Au nanoparticles located towards the crossed regions.

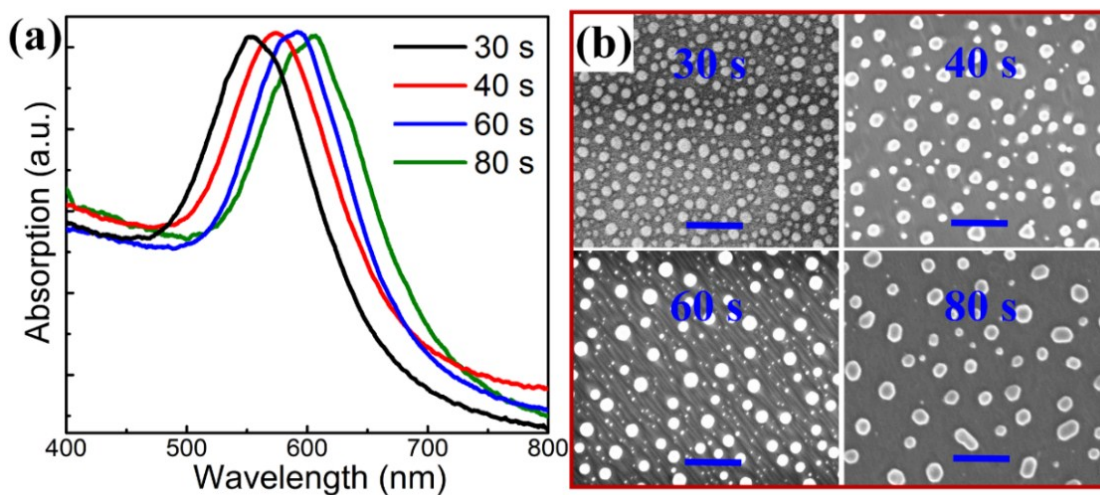


Figure S15. (a) Absorption spectra of Au nanoparticles with the sputtering times ranged from 30 s to 80s, with the peaks redshift from 550 nm to 606 nm. (b) SEM images of Au NPs with different sputtering times ranged from 30 s to 80 s.

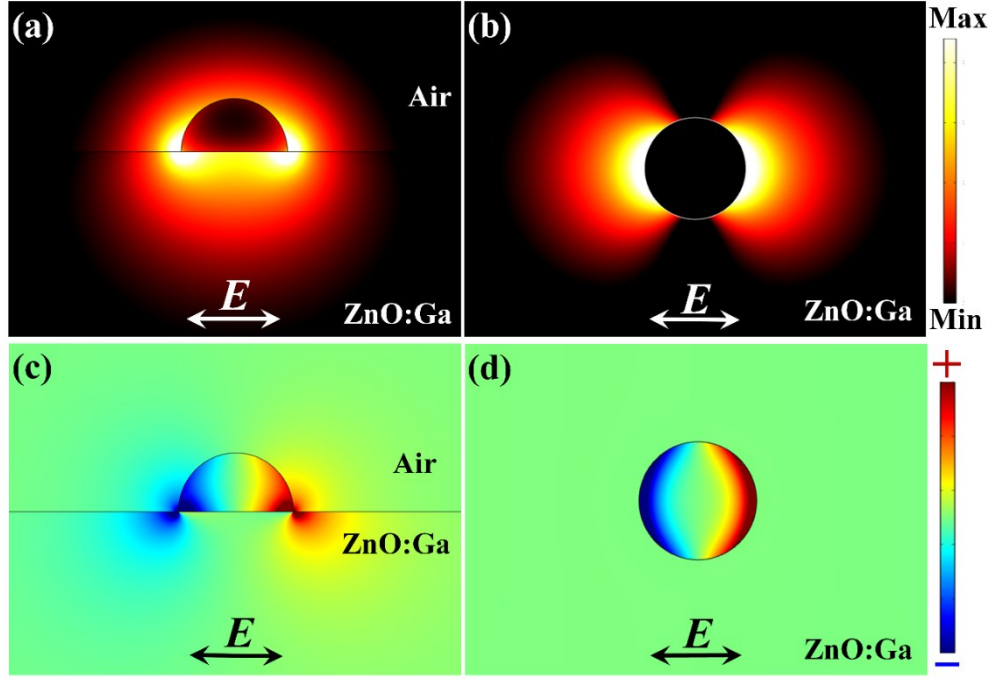


Figure S16. Spatial distribution of the electric field intensities, incident wavelength $\lambda = 600$ nm, $d = 100$ nm, two-dimensional cross section is perpendicular to the direction of incident light (a), and parallel to the direction of incident light (b), respectively. In accordance with the charge distributions (c) and (d) respectively. During the numerical simulation, incident wavelengths $\lambda=550$ nm, the diameter of Au nanoparticles denoted as $D=100$ nm, corresponding dielectric constant $\epsilon=-6.35+1.05i$.